

Article

Homogenization of Radial Temperature by a Tungsten Sink in Sublimation Growth of 45 mm AlN Single Crystal

Yue Yu, Botao Liu, Xia Tang, Sheng Liu and Bing Gao *

The Institute of Technological Sciences, Wuhan University, Wuhan 430072, China; 2019106520025@whu.edu.cn (Y.Y.); 2018106520020@whu.edu.cn (B.L.); 2018106520022@whu.edu.cn (X.T.); victorliu@whu.edu.cn (S.L.)

* Correspondence: gaobing@whu.edu.cn

Received: 9 November 2020; Accepted: 2 December 2020; Published: 6 December 2020



Abstract: To reduce the thermal stress during the sublimation growth of 45 mm AlN single crystal, a tungsten sink was put on the top of the crucible lid. Numerical experiments showed that the radial temperature gradient was reduced due to the homogenization effect on temperature as a result of the sink. Therefore, this simple tungsten sink method has the potential to grow large-size AlN ingots with fewer cracks. It also reveals that enhancing the heat exchange of the crucible lid is an effective way to improve the quality of crystal growth.

Keywords: sublimation growth; AlN single crystal; thermal stress; numerical experiments

1. Introduction

Aluminum nitride (AlN) is a promising material due to its wide band gap (6.28 eV), high thermal conductivity ($340 \text{ W}\cdot\text{m}^{-1}\cdot\text{K}^{-1}$) and small lattice and thermal expansion mismatch with GaN [1]. AlN has great potential in high-power and high-frequency electronic and deep ultraviolet (UV) optoelectronic industries [2]. AlN single crystal is usually grown by the physical vapor transport (PVT) method [3]. However, AlN crystal growth is difficult, especially in large sizes, with cracks occurring frequently [4]. To reduce the probability of crack occurrence, it is important to reduce the thermal stress by homogenizing the radial temperature distribution. There are two methods to achieve this. The first is to perform experiments using trial and error; however, this method is expensive and time consuming. The second is numerical simulation and optimization, which is low cost and highly efficient [5].

Many groups have used the second method to improve AlN crystal growth and enhance crystal quality. Liu and Edgar [6] developed a global model for simulating AlN sublimation growth that included surface kinetics. Liu [7] and Wu [8] formulated an integrated model that considered induction heating, thermal system design, mass transport and growth kinetics. Gao et al. [9] established a fully coupled compressible flow model to study the sublimation and mass transport processes in AlN crystal growth. Wang et al. [10] studied the distribution and evolution of the total resolved shear stress in AlN single crystals. Wolfson and Mokhov [11] examined the dependence of growth rate on nitrogen pressure. Segal et al. [12] developed a model that considered the diffusive and convective transport of gases and the kinetic limitation of nitrogen adsorption/desorption on AlN surfaces. Wang and Deng [13] investigated the effect of the hot-zone structure on the temperature distribution in growth chambers. Wang and Zhang [14] investigated the effect of different temperature distributions on the growth of AlN crystals through simulation and experimentation. Liu et al. [15] focused on the crystal growth mode and the defects in AlN grown on different (0001) 6H-SiC substrates and examined the effects of the substrate preparation on the growth mode and types of resultant

defects. Zhuang and Edgar [16] studied AlN single-crystal growth using a microwave-heated furnace. Hartmann [17] grew freestanding AlN single crystals with c-plane areas exceeding 10 mm in diameter. Zhang [18] used SiC heterogeneous seeds to grow AlN single crystals with a diameter of 40 mm. Hu [19] assessed the correlation of the quality of AlN layers grown on SiC seeds with the growth temperature and orientation of the seeds.

Although many numerical studies have been conducted, most were focused on the growth of AlN crystals less than 25 mm in radius; there are few studies on larger-size AlN single crystals for industrial production. The advantages of numerical simulation are the simplification of the experimental process and reduction of the difficulty of the experiment. Thus, numerical simulation and optimization are ideal for the growth of large crystals.

In this paper, numerical simulation was used to optimize the radial temperature distribution for minimizing the thermal stress of AlN crystal with a radius of 45 mm during sublimation growth. The simulation showed that a tungsten sink design placed on the top of the crucible lid can effectively improve the radial temperature distribution and reduce the thermal stress.

2. Simulation

2.1. Geometric Model

Figure 1a shows the simulated 45 mm AlN sublimation growth furnace according to traditional design. The crucible is made of tungsten and placed in a nitrogen-rich ambient. The crucible is typically 200 mm in height and 70 mm in radius. The crucible wall thickness is 20 mm. The thermal insulation is made of graphite felt. In order to simplify the calculation, the emissivity of the material is unified to 0.8. A seed 45 mm in radius and 7 mm in thickness is mounted on the bottom of the crucible lid. The growth system is heated by induction coil (10 kHz) [20,21]. Figure 1b shows the improved 45 mm growth furnace using a tungsten sink method. The sink material could also be high-density graphite with a high thermal conductivity.

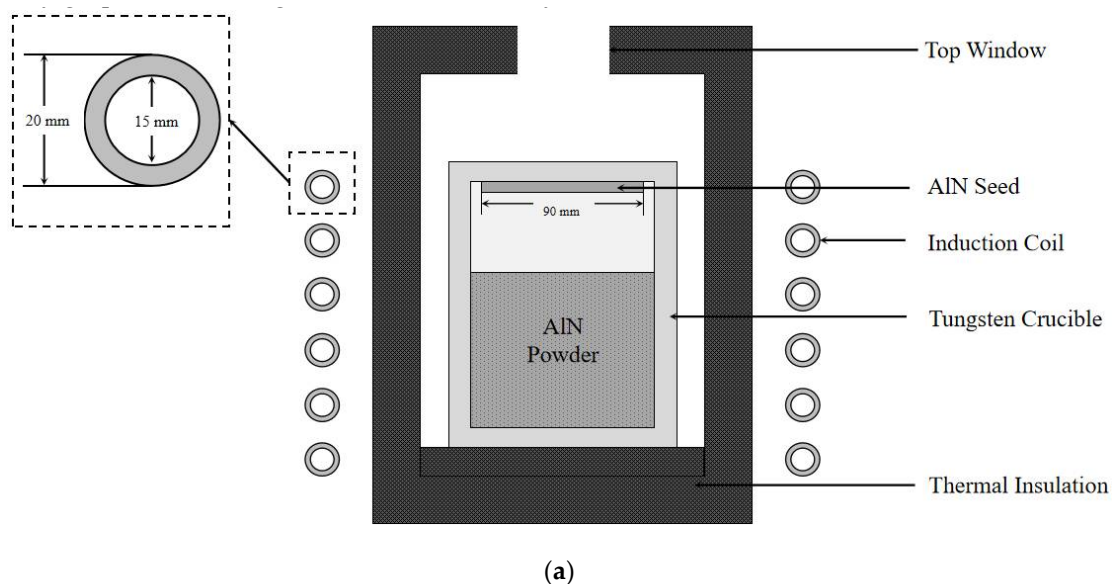


Figure 1. Cont.

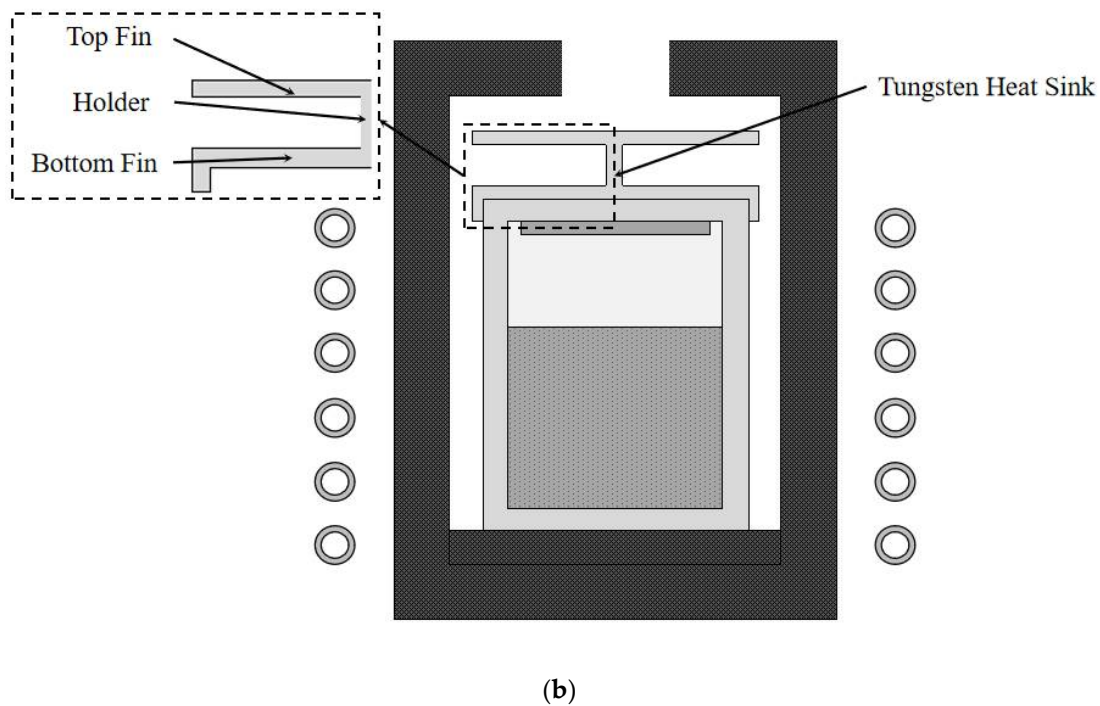


Figure 1. (a) AlN sublimation growth furnace according to traditional design; (b) AlN sublimation growth furnace according to improved design.

2.2. Mathematical Model

The governing equations and the boundary conditions of heat transfer can be expressed as [20–22]:

$$\rho C_p \frac{\partial T}{\partial t} = \nabla(k \nabla T) + q_{radi} + q_{eddy} \quad (1)$$

$$\frac{q_{radi}}{\varepsilon_j} - \sum_{k=1}^N F_{j,k} \frac{1 - \varepsilon_k}{\varepsilon_k} q_{radi,k} = \sigma T_j^4 - \sum_{k=1}^N F_{j,k} \sigma T_k^4 \quad (2)$$

$$q_{eddy} = \frac{1}{2} \sigma_c \omega^2 (A_r^2 + A_i^2) \quad (3)$$

where ρC_p is the effective heat capacity, k is the thermal conductivity, q_{radi} is the radiative heat flux on the surface of the growth chamber and q_{eddy} is the heat flux caused by the eddy current.

Table 1 shows the thermophysical properties of materials in the growth chamber [23,24].

Table 1. Thermophysical properties of materials in the growth chamber.

	Thermal Conductivity (W/m·K)	Density (kg/m ³)	Heat Capacity (J/kg·K)
Tungsten crucible	180	19,300	135
Insulation	0.5	170	2100
AlN powder	22.55	270.34	1172.7
AlN seed	320	3250	1197

The thermal stress of AlN crystal is calculated according to the following equations [25,26]:

$$\frac{1}{r} \frac{\partial}{\partial r} (r \sigma_{rr}) + \frac{\partial \tau_{rz}}{\partial z} - \frac{\sigma_{\phi\phi}}{r} = 0 \quad (4)$$

$$\frac{1}{r} \frac{\partial}{\partial r} (r\tau_{rz}) + \frac{\partial \sigma_{zz}}{\partial z} = 0 \quad (5)$$

$$\begin{pmatrix} \sigma_{rr} \\ \sigma_{\phi\phi} \\ \sigma_{zz} \\ \tau_{rz} \end{pmatrix} = \begin{pmatrix} c_{11} & c_{12} & c_{13} & 0 \\ c_{12} & c_{22} & c_{23} & 0 \\ c_{13} & c_{23} & c_{33} & 0 \\ 0 & 0 & 0 & c_{44} \end{pmatrix} \times \begin{pmatrix} \varepsilon_{rr} - \alpha_r(T - T_{ref}) \\ \varepsilon_{\phi\phi} - \alpha_\phi(T - T_{ref}) \\ \varepsilon_{zz} - \alpha_z(T - T_{ref}) \\ \varepsilon_{rz} \end{pmatrix} \quad (6)$$

where σ_{rr} , $\sigma_{\phi\phi}$ and σ_{zz} represent the normal stress; τ_{rz} represents the shear stress; c_{ij} is the elastic constant; ε_{rr} , $\varepsilon_{\phi\phi}$, ε_{zz} and ε_{rz} are the strain components; α_r , α_ϕ and α_z are the thermal expansion coefficients and T_{ref} is the reference temperature.

The boundary conditions for thermal stress calculations are as follows [27]. The top constraint to the crystal is rigid. Because there is no contact between the crystal and crucible wall, the crystal interface is stress free. The equations are solved by the 2D finite element method.

3. Results and Discussion

3.1. Temperature Distribution

In simulations, the structure of a finned heat exchanger was used to form a tungsten sink device that was placed on the top of the crucible lid. This device consisted of two fins and a holder between them. Together, they increased the heat exchange area, which was more conducive to radiate heat to the surrounding area. To better understand the effect of the sink on temperature distribution, we set up a series of simulations.

First, designs were chosen in which the bottom part of the tungsten sink covered the AlN seed diameter (A design), the crucible outer diameter (B design) and the whole crucible lid (C design) (see Figure 2).

The temperature distributions for the original and three improved designs are shown in Figure 2. In all of the improved designs, the temperature distributions were more uniform in the gas chamber and near the seed. This temperature distribution is beneficial for reducing thermal stress of the crystal.

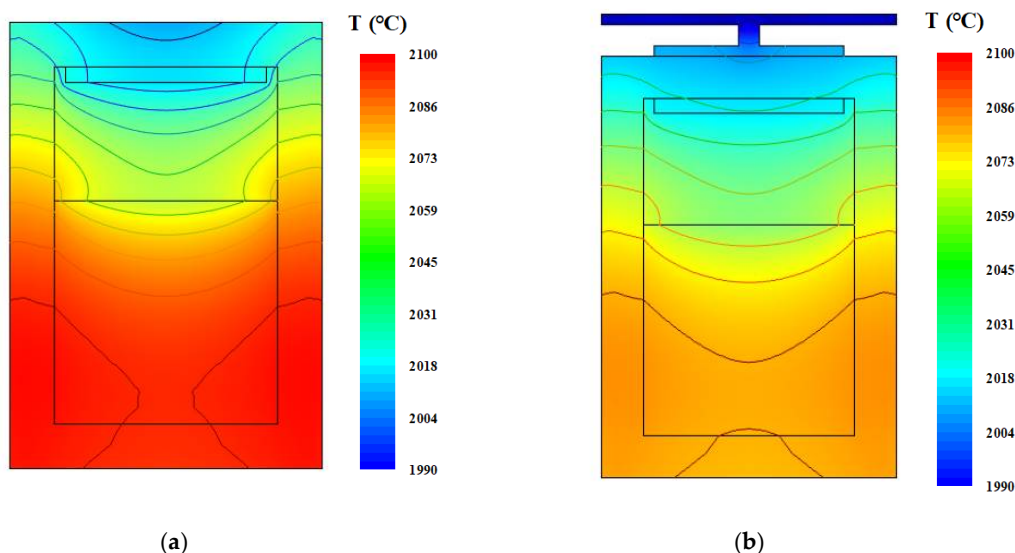


Figure 2. Cont.

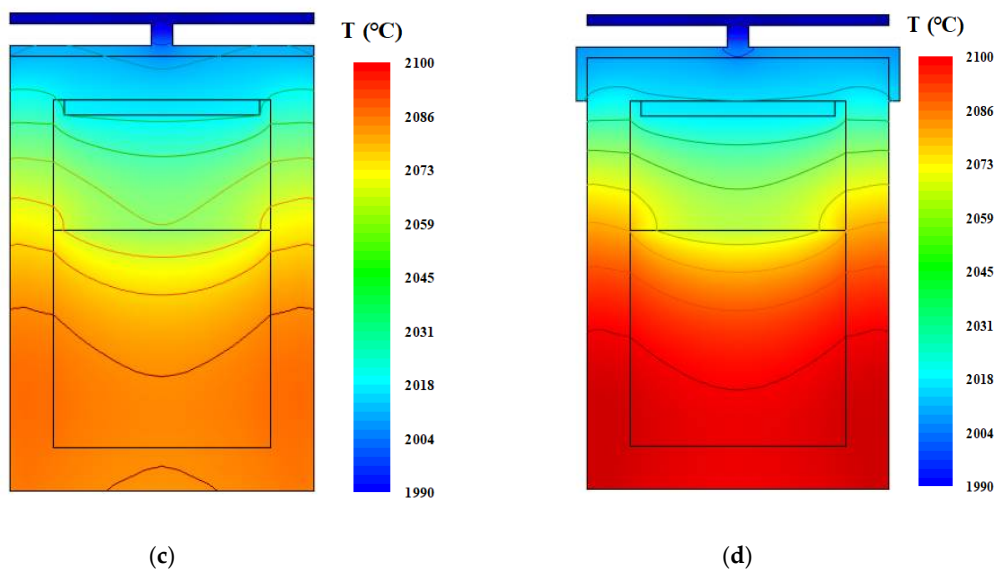


Figure 2. Temperature distributions for (a) the original design, (b) A design, (c) B design and (d) C design.

The radial temperature distributions of the AlN seed surface are shown in Figure 3. The tangent of temperature distribution (i.e., the temperature gradient) was reduced for all of the improved designs. The bottom fin created a uniform radial temperature distribution by blocking heat radiation from the crucible lid. As a result, the temperature gradient gradually decreased as the size of bottom fin gradually increased.

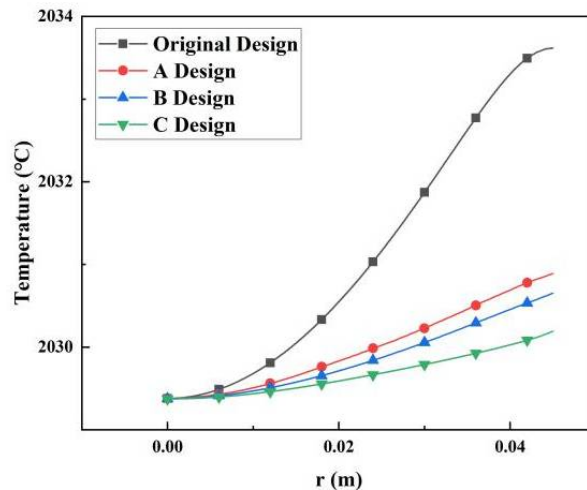


Figure 3. Radial temperature distributions of the AlN seed surface in different types of crucibles.

3.2. Temperature Gradients in Radial and Axial Directions

Figure 4 shows the temperature gradients of the original and three improved designs. Compared with the original crucible, the addition of the tungsten sink reduced both the axial and radial temperature gradient. The reduction of the axial temperature gradient decreased the growth rate, which is not beneficial for industrial production [28]. However, because of the increased heat exchange area, the axial temperature gradient increased with an increase in the bottom fin diameter. To increase the axial temperature gradient with radial temperature uniformity, the bottom fin should cover the whole crucible lid.

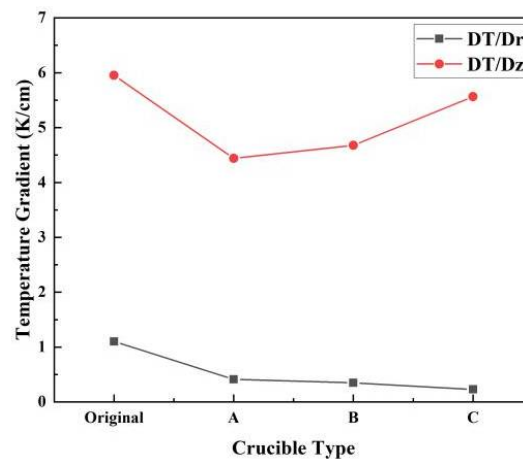


Figure 4. Temperature gradients of different types of crucibles (DT/Dr and DT/Dz represent the axial and radial temperature gradient, respectively).

To further understand the functions of the top fin, we compared the temperature gradient difference between the tungsten sink designs with and without the top fin on the bottom fin (see Figure 5). Compared with the complete tungsten sink, the heat exchange of the crucible lid was weakened with only the bottom fin present. Removing the top fin resulted in a decrease of the axial temperature gradient and an increase in the radial temperature gradient. As the radial temperature gradient is the source of thermal stress, which causes the multiplication of dislocations and leads crystal growth to failure [29], it should be as small as possible. Therefore, the bottom fin combined with a holder and a top fin is beneficial to obtain a uniform radial temperature distribution with a less-affected axial temperature distribution. In addition, it can be concluded that enhancing the heat exchange of the crucible lid is an effective way to improve the quality of crystal growth.

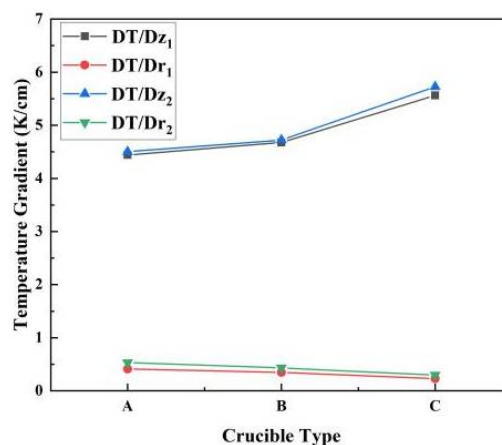


Figure 5. Comparison of temperature gradients in crucibles with different heat sinks. A, B and C designs represent designs with different bottom fin lengths; 1 and 2 represent tungsten sinks with and without the holder and top fin, respectively.

3.3. Thermal Stress in the Seed

Temperature distributions in the AlN seed are presented in Figure 6. Because of the radiation loss through the top window, the minimum temperature occurred in all designs at the center of the AlN seed top surfaces. The temperature distributions in the improved designs were greater than in the original design.

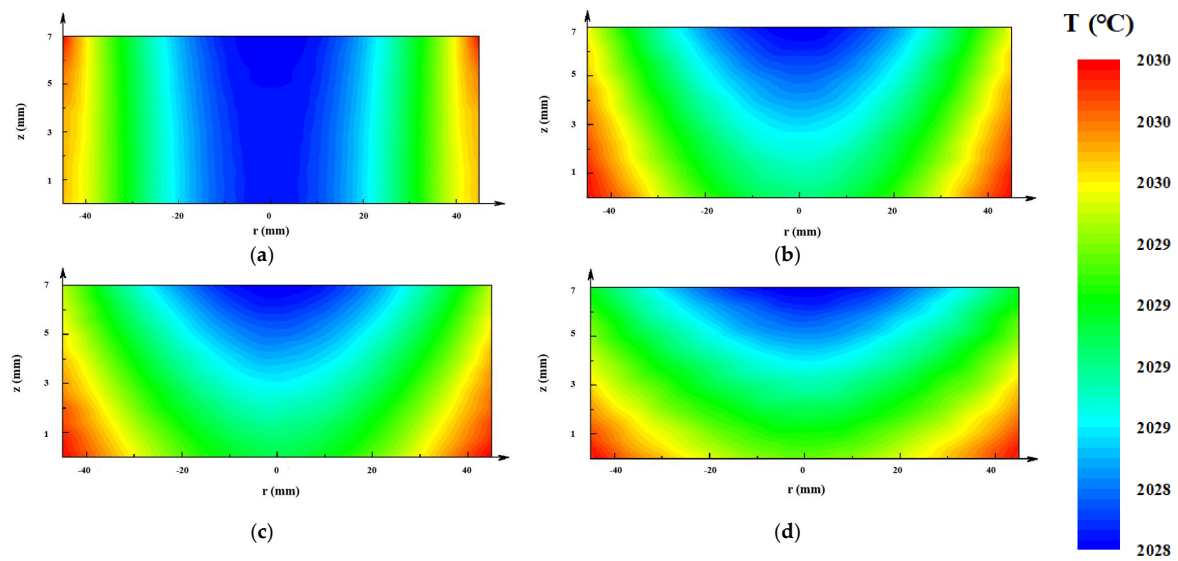


Figure 6. Temperature distributions of the AlN seed in different design crucibles: (a) original design; (b) A design; (c) B design; (d) C design.

The crystal did not contact the crucible wall. Thus, the thermal stress in the crystal was only caused by the non-uniformity of the temperature distribution. The von Mises stress is usually used as the resolved shear stress, which denotes the driving force for basal plane dislocation multiplication [30] (see Figure 7). All of the maximum thermal stresses occurred at the top periphery because of the boundary condition of the rigid top. The thermal stress in the improved designs decreased significantly compared with the original one. The minimal thermal stress appeared at the AlN crystal of the C design crucible. The thermal stress distribution also tended to be flat (see Figure 7a–d).

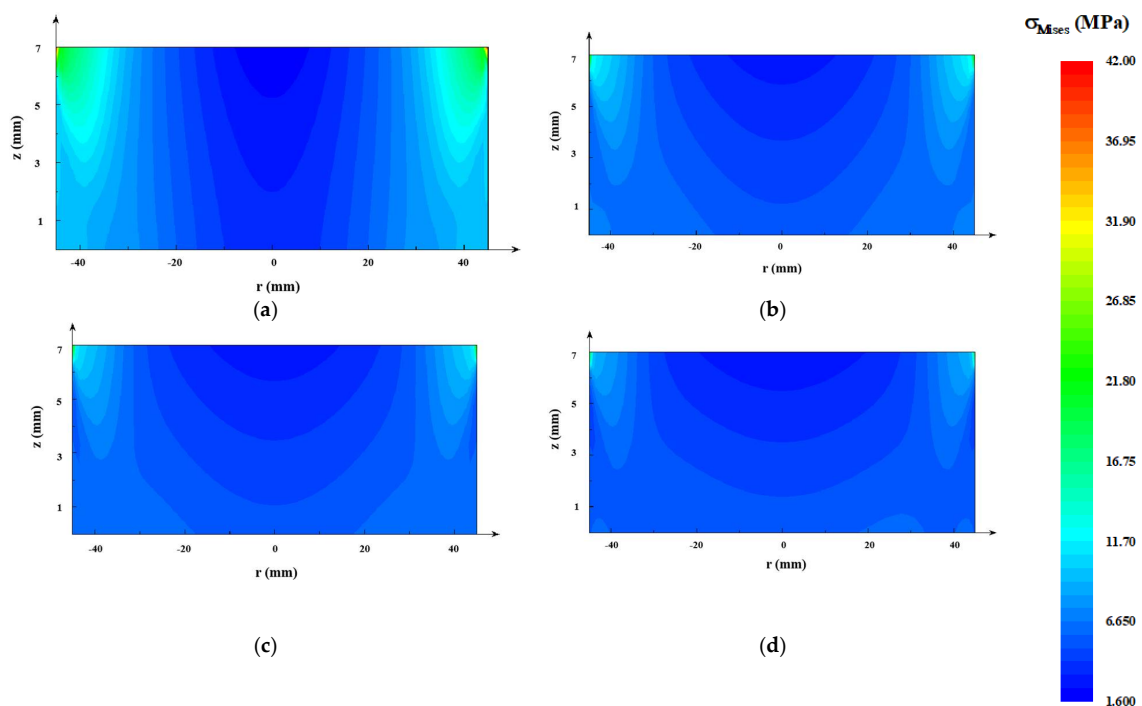


Figure 7. Thermal stress distributions of the AlN seed in crucibles with different designs: (a) original design; (b) A design; (c) B design; (d) C design.

3.4. Discussion

As can be seen in Figures 3–7, the tungsten sink design was useful for large-size AlN single crystal growth. It can reduce the radial temperature gradient and thereby reduce the thermal stress. Thermal stress causes the multiplication of dislocations and results in crystal fragmentation. An effective tungsten sink design can not only improve radial temperature distribution, but also maintain a reasonable axial temperature gradient, which means that it may reduce dislocations in crystal growth and guarantee a normal growth rate.

4. Conclusions

This study proposed the use of a tungsten sink on the top of the crucible during the sublimation growth of 45 mm AlN single crystals. Numerical experiments showed that the radial temperature gradient was reduced due to the homogenization effect of temperature by a tungsten sink. Because dislocations are one of the main problems in enlarging the size of AlN crystals, this simple tungsten sink method has great potential to grow large-size AlN ingots with reduced occurrence of cracking.

Author Contributions: Conceptualization, Y.Y.; methodology, B.G.; software, Y.Y. and B.L.; validation, S.L., X.T. and B.G.; formal analysis, Y.Y.; investigation, Y.Y.; resources, Y.Y.; data curation, Y.Y.; writing—original draft preparation, Y.Y.; writing—review and editing, Y.Y.; visualization, Y.Y.; supervision, B.G.; project administration, Y.Y.; funding acquisition, B.G. All authors have read and agreed to the published version of the manuscript.

Funding: This research received no external funding.

Conflicts of Interest: The authors declare no conflict of interest.

References

1. Rojo, J.C.; Schowalter, L.J.; Gaska, R. Growth and characterization of epitaxial layers on aluminum nitride substrates prepared from bulk, single crystals. *J. Cryst. Growth* **2002**, *240*, 508–512. [[CrossRef](#)]
2. Kato, T.; Nagai, I.; Miura, T.; Kamata, H.; Naoe, K.; Sanada, K.; Okumura, H. AlN bulk crystal growth by sublimation method. *Phys. Status Solidi C* **2010**, *7*, 1775–1777. [[CrossRef](#)]
3. Zhuang, D.; Herro, Z.G.; Schlessner, R.; Sitar, Z. Seeded growth of AlN single crystals by physical vapor transport. *J. Cryst. Growth* **2006**, *287*, 372–375. [[CrossRef](#)]
4. Wu, B.; Ma, R.; Zhang, H.; Prasad, V. Modeling and simulation of AlN bulk sublimation growth systems. *J. Cryst. Growth* **2004**, *266*, 303–312. [[CrossRef](#)]
5. Klein, O.; Philip, P. Transient temperature phenomena during sublimation growth of silicon carbide single crystals. *J. Cryst. Growth* **2003**, *249*, 514–522. [[CrossRef](#)]
6. Liu, L.; Edgar, J.H. A Global Growth Rate Model for Aluminum Nitride Sublimation. *J. Electrochem. Soc.* **2002**, *149*, G12–G15. [[CrossRef](#)]
7. Liu, L.; Edgar, J.H. Transport effects in the sublimation growth of aluminum nitride. *J. Cryst. Growth* **2000**, *220*, 243–253. [[CrossRef](#)]
8. Wu, B.; Zhang, H. Transport phenomena in an aluminum nitride induction heating sublimation growth system. *Int. J. Heat Mass Transf.* **2004**, *47*, 2989–3001. [[CrossRef](#)]
9. Gao, B.; Nakano, S.; Kakimoto, K. The impact of pressure and temperature on growth rate and layer uniformity in the sublimation growth of AlN crystals. *J. Cryst. Growth* **2012**, *338*, 69–74. [[CrossRef](#)]
10. Wang, Q.; Zhao, Y.; Huang, J.; Fu, D.; Het, G.; Wu, L. Optimization of total resolved shear stress in AlN single crystals homoepitaxially grown by physical vapor transport method. *J. Cryst. Growth* **2019**, *519*, 14–19. [[CrossRef](#)]
11. Wolfson, A.A. Dependence of the growth rate of an AlN layer on nitrogen pressure in a reactor for sublimation growth of AlN crystals. *Semiconductors* **2010**, *44*, 1383–1385. [[CrossRef](#)]
12. Segal, A.S.; Karpov, S.Y.; Makarov, Y.N.; Mokhov, E.; Roenkov, A.; Ramm, M.; Vodakov, Y. On Mechanisms of Sublimation Growth of AlN Bulk Crystals. *J. Cryst. Growth* **2000**, *211*, 68–72. [[CrossRef](#)]
13. Wang, Z.; Deng, X.; Cao, K.; Wang, J.; Wu, L. Hotzone design and optimization for 2-in. AlN PVT growth process through global heat transfer modeling and simulations. *J. Cryst. Growth* **2017**, *474*, 76–80. [[CrossRef](#)]

14. Wang, G.; Zhang, L.; Wang, Y.; Shao, Y.; Chen, C.; Liu, G.; Wu, Y.; Hao, X. Effect of Temperature Gradient on AlN Crystal Growth by Physical Vapor Transport Method. *Cryst. Growth Des.* **2019**, *19*, 6736–6742. [[CrossRef](#)]
15. Liu, L.; Liu, B.; Shi, Y.; Edgar, J.H. Growth mode and defects in aluminum nitride sublimed on (0001) 6H-SiC substrates. *MRS Internet J. Nitride Semicond. Res.* **2001**, *6*, e7. [[CrossRef](#)]
16. Zhuang, D.; Edgar, J.H.; Liu, B.; Huey, H.; Jiang, H.X.; Lin, J.; Kuball, M.; Mogal, F.; Chaudhuri, J.; Rek, Z. Bulk AlN crystal growth by direct heating of the source using microwaves. *J. Cryst. Growth* **2004**, *262*, 168–174. [[CrossRef](#)]
17. Hartmann, C.; Wollweber, J.; Dittmar, A.; Irmscher, K.; Kwasniewski, A.; Langhans, F.; Neugut, T.; Bickermann, M. Preparation of bulk AlN seeds by spontaneous nucleation of freestanding crystals. *Jpn. J. Appl. Phys.* **2013**, *52*, 8. [[CrossRef](#)]
18. Zhang, L.; Qi, H.; Cheng, H.; Jin, L.; Shi, Y. Preparation and characterization of AlN seeds for homogeneous growth. *J. Semicond.* **2019**, *40*, 102801. [[CrossRef](#)]
19. Hu, W.; Guo, L.; Guo, Y.; Wang, W. Growing AlN crystals on SiC seeds: Effects of growth temperature and seed orientation. *J. Cryst. Growth* **2020**, *541*, 125654. [[CrossRef](#)]
20. Dupret, F.; Nicodeme, P.; Ryckmans, Y.; Wouters, P.; Crochet, M. Global modelling of heat transfer in crystal growth furnaces. *Int. J. Heat Mass Transf.* **1990**, *33*, 1849–1871. [[CrossRef](#)]
21. Chen, Q.S.; Zhang, H.; Prasad, V.; Balkas, C.M.; Yushin, N.K. Modeling of heat transfer and kinetics of physical vapor transport growth of silicon carbide crystals. *J. Heat Transf.* **2001**, *123*, 1098–1109. [[CrossRef](#)]
22. Li, H.; Liu, X.; Feng, Y.; Wei, H.; Yang, S. Numerical study of radial temperature distribution in the AlN sublimation growth system. *Cryst. Res. Technol.* **2013**, *48*, 321–327. [[CrossRef](#)]
23. Cai, D.; Zheng, L.; Zhang, H.; Zhuang, D.; Herro, Z.; Schlessner, R.; Sitar, Z. Effect of thermal environment evolution on AlN bulk sublimation crystal growth. *J. Cryst. Growth* **2007**, *306*, 39–46. [[CrossRef](#)]
24. Wu, B.; Ma, R.; Zhang, H.; Dudley, M.; Schlessner, R.; Sitar, Z. Growth kinetics and thermal stress in AlN bulk crystal growth. *J. Cryst. Growth* **2003**, *253*, 326–339. [[CrossRef](#)]
25. Jordan, A.S.; Caruso, R.; VonNeida, A.R. A comparative study of thermal stress induced dislocation generation in pulled GaAs, InP, and Si crystals. *J. Appl. Phys.* **1981**, *52*, 3331–3336. [[CrossRef](#)]
26. Ma, R.; Zhang, H.; Ha, S.; Skowronski, M. Integrated process modeling and experimental validation of silicon carbide sublimation growth. *J. Cryst. Growth* **2003**, *252*, 523–537. [[CrossRef](#)]
27. Ma, R.; Zhang, H.; Prasad, V.; Dudley, M. Growth kinetics and thermal stress in the sublimation growth of silicon carbide. *Cryst. Growth Des.* **2002**, *2*, 213–220. [[CrossRef](#)]
28. Meyer, C.; Philip, P. Optimizing the temperature profile during sublimation growth of SiC single crystals: Control of heating power, frequency, and coil position. *Cryst. Growth Des.* **2005**, *5*, 1145–1156. [[CrossRef](#)]
29. Meduoye, G.O.; Bacon, D.J.; Evans, K.E. Computer modelling of temperature and stress distributions in LEC-grown GaAs crystals. *J. Cryst. Growth* **1991**, *108*, 627–636. [[CrossRef](#)]
30. Gao, B.; Kakimoto, K. Three-dimensional modeling of basal plane dislocations in 4H-SiC single crystals grown by the physical vapor transport method. *Cryst. Growth Des.* **2014**, *14*, 1272–1278. [[CrossRef](#)]

Publisher's Note: MDPI stays neutral with regard to jurisdictional claims in published maps and institutional affiliations.



© 2020 by the authors. Licensee MDPI, Basel, Switzerland. This article is an open access article distributed under the terms and conditions of the Creative Commons Attribution (CC BY) license (<http://creativecommons.org/licenses/by/4.0/>).